Microbiome

RESEARCH

Open Access

High-throughput analysis of microbiomes in a meat processing facility: are food processing facilities an establishment niche for persisting bacterial communities?

Zhaohui S. Xu[1], Vi D. Pham[1], Xianqin Yang[2] and Michael G. Gänzle[1,3*]

Abstract

Background Microbial spoilage in meat impedes the development of sustainable food systems. However, our understanding of the origin of spoilage microbes is limited. Here, we describe a detailed longitudinal study that assesses the microbial dynamics in a meat processing facility using high-throughput culture-dependent and culture-independent approaches to reveal the diversity, dispersal, persistence, and biofilm formation of spoilage-associated microbes.

Results Culture-dependent and culture-independent approaches revealed a large diversity of microbes within the meat facility, including 74 undescribed bacterial taxa and multiple spoilage-associated microbes. Ten out of 10 reconstituted microbial communities formed biofilms, and the biofilm biomass was generally higher at 4 °C than at 25 °C. Isolates obtained at different sampling times or from different sampling sites that differed in fewer than 10 genome-wide single-nucleotide polymorphisms were considered the same (persistent) strains. Strains of *Carnobacterium maltaromaticum* and *Rahnella rivi* persisted over a period of 6 months across sampling sites and time, stemming from floor drains in the cooler room. Meat isolates of *Carnobacterium divergens*, *Rahnella inusitata*, and *Serratia proteamaculans* originated from food contact and non-food contact environments of the packaging area.

Conclusions Culture-dependent isolation, complemented by culture-independent analyses, is essential to fully uncover the microbial diversity in food processing facilities. Microbial populations permanently resided within the meat processing facility, serving as a source of transmission of spoilage microbes. The ability of these microbes to coexist and form biofilms facilitates their persistence. Our data together with prior data on persistence of *Listeria monocytogenes* indicates that microbial persistence in food processing facilities is the rule rather than an exception.

Keywords Meat spoilage, Multispecies biofilm, Persistence, *Listeria*, Food processing facility, Food sustainability, *Carnobacterium*, *Leuconostoc*, *Latilactobacillus*, *Pseudomonas*, *Dellaglioa*

*Correspondence:
Michael G. Gänzle
mgaenzle@ualberta.ca
[1] Department of Agricultural, Food and Nutritional Science, University of Alberta, Edmonton, AB, Canada
[2] Agriculture and Agri-Food Canada, Lacombe, AB, Canada
[3] School of Bioengineering and Food, Hubei University of Technology, Wuhan, People's Republic of China

Background

Global food systems are challenged to meet the rising demand for food while ensuring environmental sustainability in the face of climate change, population growth, and malnutrition [1]. Food waste due to microbial spoilage exacerbates these challenges. In 2019, approximately 77.4 million tonnes of pork, poultry, beef, or mutton were discarded, from which 20% was occurring during processing and packaging stages [1]. The food industry is thus prioritizing efforts to combat spoilage microbes and mitigate their adverse impacts on products' shelf life and quality.

The introduction of spoilage microbes onto meat products can occur from bacteria carried by the animals at slaughter, from the environment, or from microbes residing in the processing facility environment [2]. Major spoilage microbes on fresh meat include *Pseudomonas* species, psychrotrophic Enterobacteriaceae, and psychrotrophic lactic acid bacteria including *Carnobacterium*, *Latilactobacillus*, and *Leuconostoc* [3]. Muscle tissue is generally considered sterile, but the environment during slaughtering and fabrication are not, leading to microbial contamination with air, water, workers, and the processing environment as vectors [4]. Permanent establishment of microbes in processing environments is supported by biofilm formation [5]. Many of the typical meat spoilage bacteria including *Pseudomonas*, *Aeromonas*, Enterobacteriaceae, and *Carnobacterium* as well as the pathogenic *Listeria monocytogenes* include biofilm-forming strains, but biofilms in food processing facilities generally are multispecies biofilms that also support integration of (pathogenic) bacteria that do not form biofilms in pure culture [6–8]. Biofilm-embedded bacteria attach to the surface of equipment or the processing rooms. The protective barrier of the biofilm matrix and the development of persister cells under nutrient-deficient conditions increases bacterial resistance to sanitizers [9, 10]. The food industry controls biofilm formation by hygienic design of processing equipment and facilities; however, these efforts fail to fully control the problem, and some microbes persist in food processing facilities. This is best documented for pathogenic bacteria. For example, a Canadian listeriosis outbreak in 2008 was attributed to *L. monocytogenes* persisting inside of a slicing machine [11] where they were not eradicated by routine sanitization measures.

Current studies on the composition of microbial communities in food processing facilities are predominantly based on high-throughput sequencing of 16S rRNA gene amplicons [6, 12] or metagenomic sequencing [8]. This approach identifies microbial taxa at the species or genus level; however, many bacterial activities and characteristics are strain dependent. For example, different strains of *Carnobacterium maltaromaticum* exhibited different spoilage-related activities and were affected differently by storage conditions [13]. While metagenomic sequencing can provide strain level information [14, 15], SNP calling of high-quality genome sequences of isolates remains the gold standard of strain-level identification. This approach is routinely used in outbreak investigations to identify the transmission paths of bacterial pathogens [16].

The assessment of long-term persistence of microbes in food processing facilities allows differentiation whether these facilities constitute an establishment niche or a persistence niche. An establishment niche is defined as a niche where bacterial populations persist without dispersal from other sources. A persistence niche is defined as a niche where growth is slower than inactivation, and the presence of bacterial populations is observed only if they recurrently transmit from other sources [17]. Current data on strain-level bacterial persistence on farms or in food processing plants is limited to foodborne pathogens such as *L. monocytogenes* [18–20], *Salmonella* [21], and *Escherichia coli* O157:H7 [22]. Not only spoilage microbes do contribute to food deterioration but also the biofilms formed by these microbes also enable the persistence of microbes that do not form biofilms and may shelter foodborne pathogens [6, 23]. The strain-level persistence of spoilage microbes, however, has not yet been described. Therefore, this study aimed to use high-throughput cultivation to characterize microbial communities in a meat processing facility. The strain-level characterization allowed to determine the overlap between isolates from different sites and meat products at two sampling times over a 6-month period. Isolates were also used to reconstitute multispecies biofilms to assess their biofilm formation and composition.

Results

High-throughput culture-dependent and culture-independent characterization of microbial communities in the meat processing facility

We used culture-dependent and culture-independent methodologies to characterize the microbial communities in the processing facility (Fig. 1). The culture-dependent approach used PCA, APT, and VRBG agars to enumerate total aerobic bacteria, lactic acid bacteria, and Enterobacteriaceae. From the 46 and 73 samples taken during the first (Sept 2022) and second sampling (Mar 2023), the number of meat samples, food contact surfaces, and non-food contact surfaces for each sampling is shown in Fig. 1. Tables S1 and S2 provide a detailed list of all sites that were sampled in each round. A total of 739 and 1435 isolates were obtained in the first and the second sampling, respectively. Of these, 605 nonredundant isolates from the first sampling and 1281 nonredundant

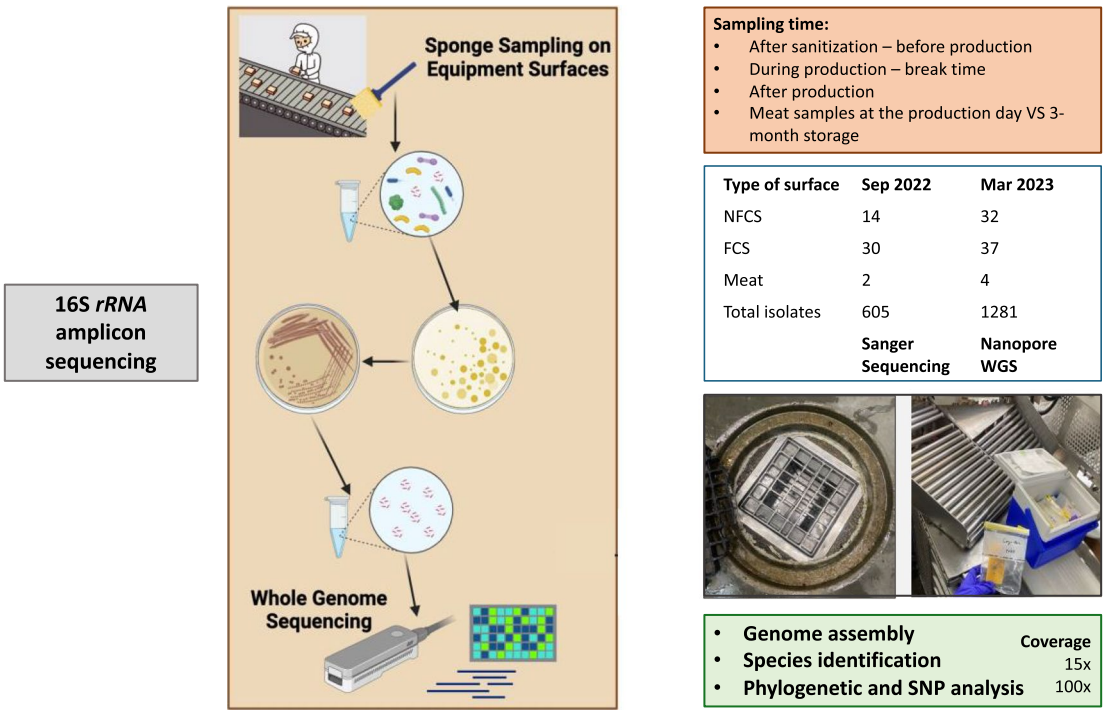

Fig. 1 Overview on the sampling strategy and experimental workflow used in this study. FCS, food contact surfaces; NFCS, non-food contact surfaces. The images to the lower right show a floor drain and parts of a conveyor belt

isolates from the second sampling were characterized at the species level by Sanger sequencing of the full-length 16S rRNA gene and nanopore whole genome sequencing, respectively (Fig. 2 and Fig. S1). Because of the more comprehensive sampling and analysis of isolates that were obtained in the second sampling, emphasis is placed on results of the second sampling. Selected isolates that were obtained in the first sampling were also genome sequenced to allow identification of persistent isolates (see below).

The microbial diversity in meat samples at the time of packaging was similar for both sampling times, and lactic acid bacteria (*Carnobacterium* and *Latilactobacillus* spp.), Enterobacterales (*Hafnia*, *Rahnella*, and *Serratia* spp.), and *Pseudomonas* spp. were consistently isolated. *Pseudomonas* species were the most prevalent in meat and environmental samples, regardless of whether the sample was from surfaces before or after sanitation (Fig. 2 and Fig. S1). Other frequent isolates include Enterobacteriaceae, *Janthinobacterium*, *Psychrobacter*, *Acinetobacter*, and *Flavobacterium*. Gram-positive organisms including lactic acid bacteria, staphylococci, and *Brochothrix* only accounted for a small fraction of the total number of isolates (Fig. 2 and Fig. S1). The microbial composition in the drain (cooler) after cleaning and sanitation, trolley (cooler), and tray (fabrication room) during production overlapped with that of meat collar samples. Most bacterial species that were isolated from samples taken during production were also isolated after sanitation (Fig. 2 and Fig. S1). Several genera including *Acinetobacter*, *Janthinobacterium*, *Psychrobacter*, and *Serratia*, however, were not recovered from sanitized surfaces, although these were highly prevalent during operation. After 90 days of vacuum-packaged refrigerated storage, meat microbiota changed, and facultative anaerobes including *Carnobacterium*, *Lactococcus*, *Leuconostoc*, and *Latilactobacillus* species and Enterobacterales of the genera *Rahnella*, *Hafnia*, *Serratia*, *Yersinia*, and *Rouxiella* dominated. Pathogens were not detected, but the nonpathogenic *Listeria welshimeri* was found on the inner surface of connection joints of a conveyor belt (D-BT3 CI).

Each sample was additionally characterized by sequencing of full-length 16S rRNA gene amplicons to identify uncultured organisms (Fig. 3 and Fig. S2). Of 4 out of 70 samples collected in March 2023, the biomass was too low to obtain PCR amplicons. In 54 of the remaining 66 samples, more than 75% of the bacterial diversity at the genus level identified by 16S rRNA gene amplicons was captured through culturing. In six samples, culture-based methodology accounted for less than 25% of the genera identified by sequencing (Fig. 3). The proportion of uncultured organisms was particularly high on sanitized surfaces where dead microbial cells are

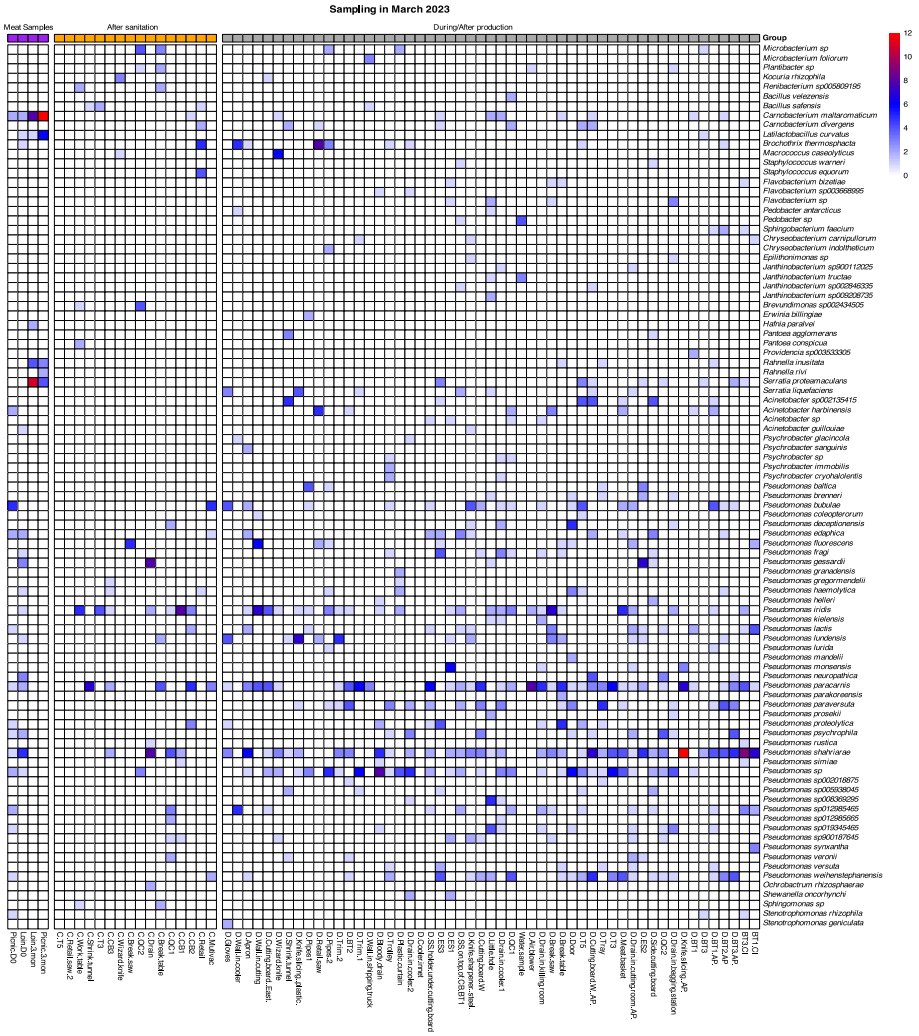

Fig. 2 Heatmap of bacterial isolates collected from meat samples and environmental surface samples during the second time sampling, March 2023. Taxonomy classification was determined based on whole-genome pairwise alignment to Genome Taxonomy Database. The sample codes are explained in more detail in online supplementary Table S2. The following taxa were detected only once and are not shown: *Hafnia alvei* and *Moellerella* sp. in loin 3mon; *Methylobacterium* sp. in C-work table; *Neobacillus* sp002559145 in C-CB3, *Aerococcus viridans* and *Staphylococcus saprophyticus* in C-wizard knife; *Macrococcus* sp019357535 in C-retail; *Frigoribacterium* sp001421165 and *Psychrobacter maritimus* in D-wall in cooler; *Pseudochrobactrum* sp. in D-Apron; *Janthinobacterium* sp002878455 in D-wizard knife; *Pseudomonas extremaustralis* in D-Shrink tunnel; *Pseudomonas* sp002874965 in D-pipes 1; *Bacillus altitudinis*, *Priestia megaterium*, *Enterococcus viikkiensis*, and *Pigmentiphaga litoralis* in D-wall in shipping truck; *Yersinia intermedia* in D-Bloody drain; *Pseudoclavibacter* sp. and *Variovorax* sp. in D-plastic curtain; *Specibacter* sp. and *Shewanella glacialipiscicola* in D-drain in cooler 2; *Serratia* sp. in D-side cutting board; *Aeromonas salmonicida* and *Pseudomonas mohnii* in D-ES1; *Stenotrophomonas* sp. in D-knife sharpener (plastic); *Sphingobacterium* sp000938735, *Microbacterium* sp002979655, and *Pseudomonas* sp010095445 in D-drain in cooler 1; *Polaromonas* sp. in water sample, *Janthinobacterium* sp009923995 in D-break table; *Pseudomonas taetrolens* in D-door, *Pseudomonas cremoris* in D-Trim 5 (T5); *Janthinobacterium* sp. in D-drain in cutting room; *Paeniglutamicibacter antarcticus*, *Flavobacterium frigidimaris*, *Acinetobacter albensis*, and *Pseudomonas tritici* in D-drain in bagging station; *Pseudomonas koreensis* in D-BT3 (AP); *Listeria welshimeri*, *Morganella* sp., and *Buttiauxella massiliensis* in D-BT3 CI; and *Serratia fonticola* in D-BT1 CI. Isolates are designated with sp# if a matching sequence is available in the GTDB but the species has not been formally described; taxa are designated with sp. if no sequence with *ANI* > 95% was available on the GTDB

present. Additionally, our culture-based approach did not recover strict anaerobes. Low abundance taxa in nutrient-deficient surfaces such as pipes, curtain, and walls were also identified with sequencing but not with culturing. The higher proportion of uncultured genera among samples collected in September 2022 (Fig. S2) may relate to the smaller number of isolates collected. The genera *Janthinobacterium*, *Paraburkholderia*, *Brevundimonas*, *Devosia*, and *Dellaglioa* were underrepresented or not recovered by culture but accounted for a substantial

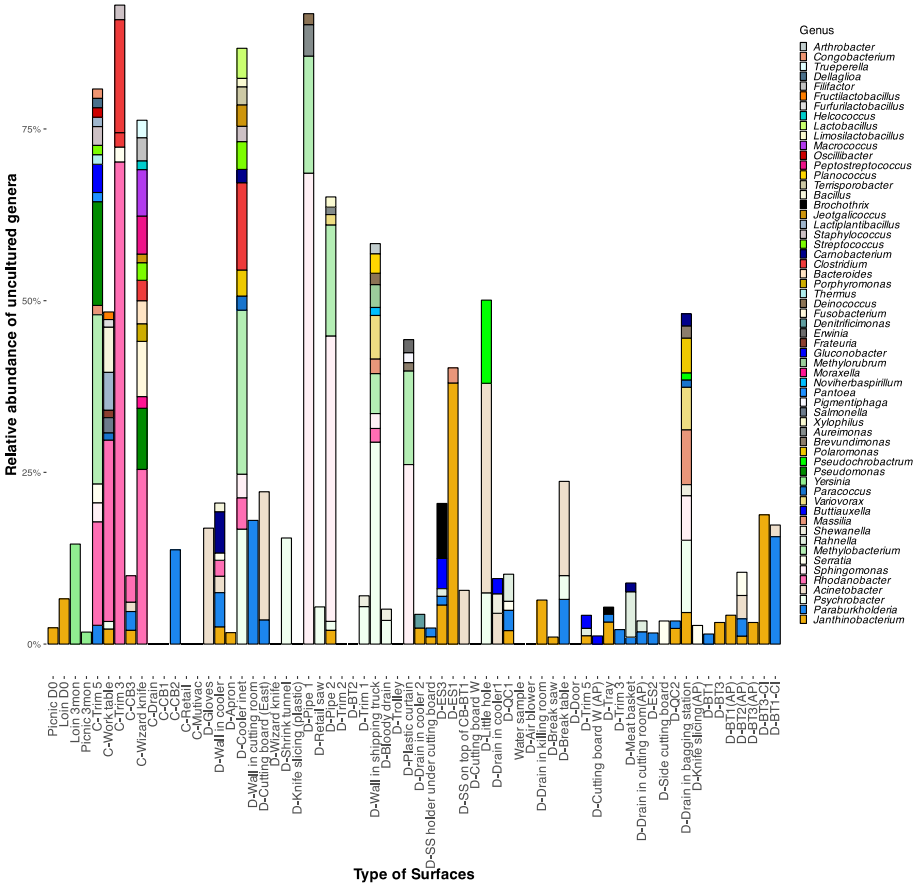

Fig. 3 Relative abundance of uncultured genera identified in samples collected in March 2023 by sequencing of full-length 16S rRNA genes. Genera with a relative abundance less than 1% are not shown. Sampling sites without a stacked bar indicates all genera was recovered by surface plating

proportion of sequences in several samples (Fig. 3 and Fig. S2).

Conversely, multiple taxa were frequently cultured but represented less than 1% of the 16S rRNA gene sequences or were not represented (Table 1). Only one sequencing read (out of 15,122 reads) was classified as *Listeria*, but *L. welshimeri* was isolated from a conveyor-related surface.

Microbial diversity in the meat processing facility

Both culture-dependent and culture-independent approaches revealed diverse microbial communities in the meat processing facility. A collection of 1885 isolates from two sampling periods represented 4 phyla: *Pseudomonadota*, *Bacillota*, *Bacteroidota*, and *Actinomycetota*. During the first sampling, 28 genera and 76 species were cultured; during the second sampling, 47 genera and 137 species were identified (Fig. 2 & Fig. S1). Multiple isolates from the second sampling could not be assigned to known species in the GTDB, indicating isolation of 74 novel taxa (Fig. 2). These isolates are designated as "sp." or "sp" followed by numbers. The culture-independent approach identified 67 and 68 genera with a relative abundance of 1% or higher in September 2022 and March 2023, respectively. Among these, 23 genera were identified in both sampling times.

The composition of microbial communities on meat and environmental samples was analyzed with the Bray–Curtis distance across four classifications: (i) type of surfaces, (ii) location, (iii) zone concept based on the proximity to food products [24], and (iv) pre- and post-sanitation. Analyses, conducted based on both culture-dependent and culture-independent approaches, showed significant ($p < 0.05$, Table S3) differences in the surface microbiome before and after sanitation. The differentiation based on surface type, location, or classified zone at either sampling time did not reveal significant differences (Fig. 4, Fig. 5, Fig. S3, and Table S3). This suggests that the microbial communities at different sites in the processing facility are similar to each other. In all analyses, the composition of microbial communities on meat overlapped

Table 1 Bacterial isolates that represented less than 1% of the respective genera in nanopore 16S rRNA gene sequencing or were not detected by sequencing

Isolates at genus level	No. of species	Sampling sites
Acinetobacter	1	D-knife sharpener steel
Aerococcus	1	C-wizard knife
Bacillus	2	C-retail, D-QC1
Brevundimonas	1	C-work table
Brochothrix	1	D-apron, D-trolley, D-BT2(AP[a]), loin D0
Carnobacterium	2	C-retail, D-cutting board W (AP), D-QC1, D-retail saw, D-shrink tunnel C-CB2, D-wizard knife, D-break table, D-BT1, D-BT2(AP), D-cutting board W (AP), D-drain in cooler 1, D-little hole (floor trap), loin D0, Picnic D0
Chryseobacterium	2	BT1-CI, D-Trim 1, D-knife sharpener steel, D-pipes 2
Enterococcus	1	D-wall in shipping truck
Epilithonimonas	1	D-drain in bagging station, D-knife sharpener steel
Erwinia	1	D-pipes 1
Flavobacterium	3	BT3-CI, D-break saw, D-break table, D-ES1, D-bloody drain
Frigoribacterium	1	D-wall in cooler
Janthinobacterium	2	D-ss on top of CB BT1, D-wizard knife
Kocuria	1	C-wizard knife, D-cutting board East
Latilactobacillus	1	D-BT3, loin D0, Picnic.3.mon
Listeria	1	BT3-CI
Macrococcus	1	C-retail
Microbacterium	3	D-wall in shipping truck, D-BT3, D-pipes 2, plastic-curtain, D-drain in cooler 1
Moellerella	1	Loin 3mon
Morganella	1	BT3-CI
Neobacillus	1	C-CB3
Ochrobactrum	1	C-drain
Paeniglutamicibacter	1	D-drain in bagging station
Pantoea	2	D-shrink tunnel, D-side cutting board, C-work table
Pedobacter	2	D-wall in cooler, D-ss on top of CB BT1
Pigmentiphaga	1	D-wall in shipping truck
Plantibacter	1	C-break table, D-air blower, D-drain in bagging station
Polaromonas	1	Water sample
Priestia	1	D-wall in shipping truck
Providencia	1	D-BT1
Pseudoclavibacter	1	Plastic curtain
Pseudomonas	1	C-retail
Psychrobacter	2	D-apron, D-QC1
Rahnella	1	D-break table
Renibacterium	1	C-work table
Serratia	4	BT1-CI, D-gloves, D-drain in cutting room AP, D-knife slicing plastic, D-little hole (floor trap), D-ss on top of CB BT1, BT3-CI, D-BT3, D-BT3(AP), D-QC2, D-ss holder under cutting board
Specibacter	1	Drain in cooler 2
Sphingobacterium	3	BT3-CI, D-BT1(AP), D-BT2(AP), C-work table, D-drain in cooler 1
Staphylococcus	3	C-retail, C-wizard knife, D-side cutting board, D-ss on top of CB BT1
Stenotrophomonas	3	D-gloves, BT3-CI, D-BT3, Picnic D0, D-knife sharpener steel
Yersinia	1	D-bloody drain

[a] Sampling sites flagged with "AP" represent sample collected after production

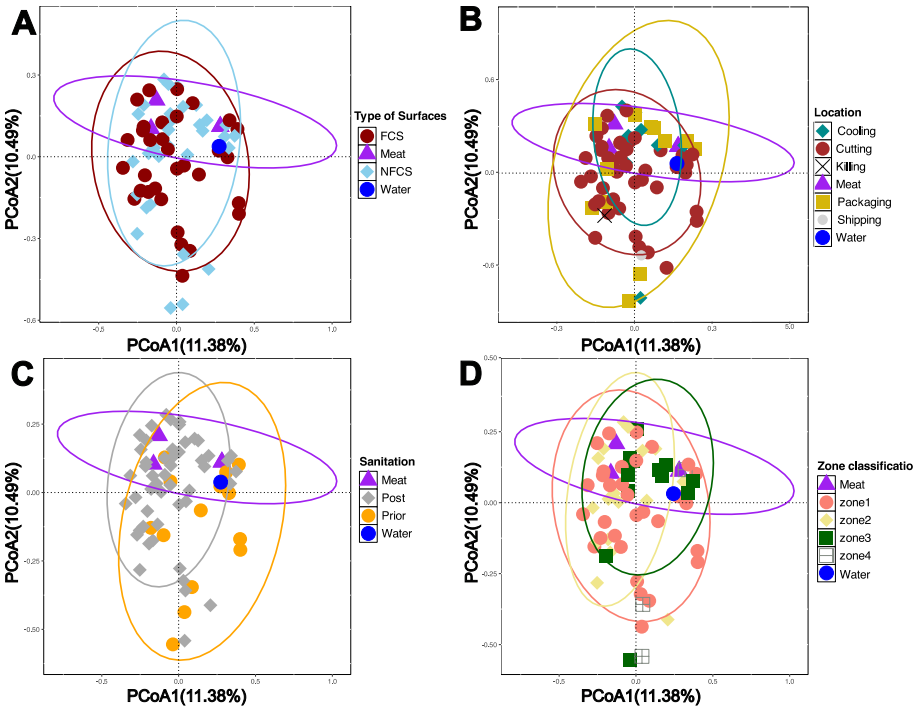

Fig. 4 Principal coordinate analysis, using Bray–Curtis distance with isolates classified at species level for 70 sampling sites, collected in March 2023. The dissimilarity among collected samples was measured from four categories: **A** Type of surfaces, **B** location, **C** sanitation activity, and **D** zone classification. Permutational multivariate analysis of variance was used to statistically differentiate among the bacterial communities. PERMANOVA results indicated that surface type ($R^2 = 0.0748$, $p = 0.001$), location ($R^2 = 0.13084$, $p = 0.001$), sanitation activity ($R^2 = 0.09032$, $p = 0.001$), and zone classification ($R.^2 = 0.11816$, $p = 0.001$) significantly contributed to bacterial community variation. The associations of community variance with different categories are displayed in Supplementary Table S3

with the composition of microbial communities on food contact and non-food contact surfaces in the facility.

Bacterial interactions on meat processing environmental and meat surfaces

Bacterial correlation networks of isolates and 16S rRNA gene amplicons obtained in March 2023 were constructed to explore patterns of bacterial co-occurrence (Fig. 6 and Fig. S4). The positive correlations between species suggest synergistic relationships and possibly preferences for similar growth conditions, contamination patterns, or surrounding environments [2]. The analysis based on culture-independent approach identified multiple clusters with species of the genera *Psychrobacter*, *Janthinobacterium*, *Pseudomonas*, *Acinetobacter*, and *Pantoea* at the center (Fig. 6). Spoilage-associated microorganisms such as *Carnobacterium* and *Latilactobacillus* co-occurred with gram-negative organisms (Fig. 6 and Fig. S4). Most *Pseudomonas* species correlated with others, implying the synergistic interspecies interactions in the meat processing environment. *Janthinobacterium* displayed positive correlations with *Serratia liquefaciens*, *Pseudomonas*, and *Pedobacter* species (Fig. 6). Co-occurrence patterns among several novel species imply their unique ecological roles. The network analysis based on 16S rRNA genes identified three clusters: one large cluster and two smaller ones (Fig. S4) and only partially overlapped with the species-level interactions (Fig. 6).

Biofilm formation

To determine the ability of the microbial communities to form biofilms, we reconstituted isolates of 10 sampling sites to obtain communities with 5–15 species. All microbial communities formed biofilms with a crystal violet absorption ranging from 0.4 to 2.4 after 6-day incubation. Microbial communities from stored meat showed weakest biofilm formation (Fig. 7A). Multispecies biofilms had a significantly higher biomass at 4 °C than at 25 °C, except for mixed cultures from the clean drain (Fig. 7E). The highest biomass (2.40 ± 0.29) occurred in a sample grown at 4 °C (Fig. 7K).

Temperature altered the biofilm community composition and the type of biofilms. Overall, a high temperature (25 °C) favored the growth of *Carnobacterium* species (Fig. 7). In contrast, the abundance of *Serratia*

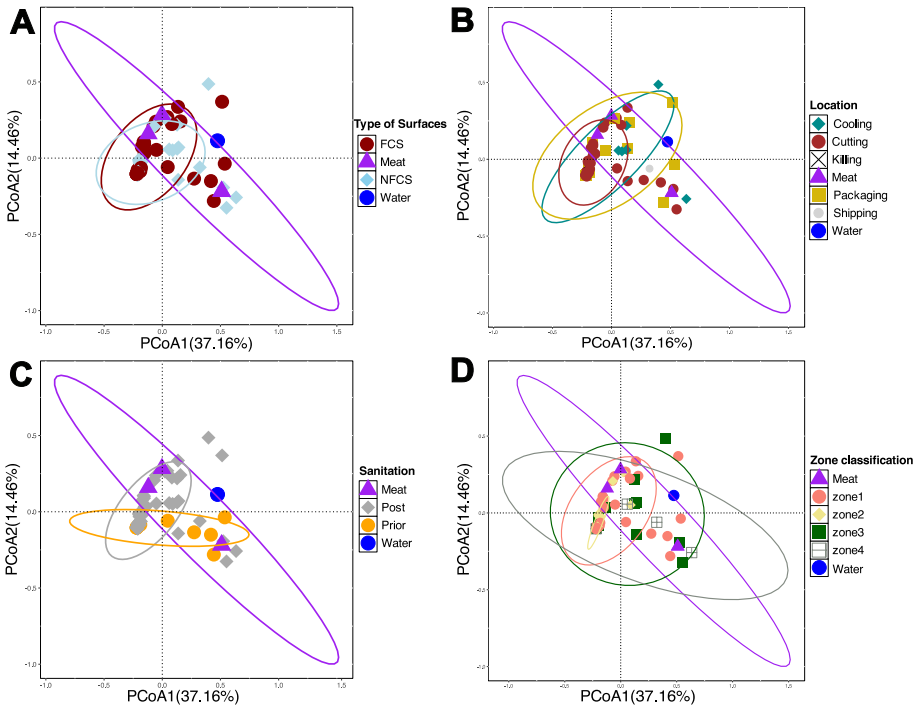

Fig. 5 Principal coordinate analysis (PCoA) plots of the Bray–Curtis distance matrix for bacteria community as determined by 16S rRNA amplicon sequencing of samples from March 2023. The samples were grouped based on surface type (**A**), location (**B**), sanitation activity (**C**), and zone classification (**D**). Permutational multivariate analysis of variance was used to statistically differentiate among the bacterial communities. PERMANOVA results indicated that surface type ($R^2 = 0.14286$, $p = 0.003$), location ($R^2 = 0.20647$, $p = 0.003$), sanitation activity ($R^2 = 0.16204$, $p = 0.001$), and zone classification ($R.^2 = 0.23427$, $p = 0.001$) significantly contributed to bacterial community variation. The associations of community variance with different sample groups are displayed in Supplementary Table S3

species was independent of incubation temperature (Fig. 7). *Leuconostoc gelidum* (Fig. 7F and H), *Lt. curvatus* (Fig. 7G), *Duganella zoogloeoides* (Fig. 7C), and *Pedobacter antarcticus* (Fig. 7D) were not detected in multispecies biofilms regardless of incubation temperature. Pellicles were formed by the microbial community isolated from fresh meat at 4 °C but not at 25 °C.

The microbial composition of biofilm examined by culturing and 16S rRNA sequencing revealed agreement on the diversity and abundance (Fig. 7B-K and Table S4). Prevalent genera included *Carnobacterium*, *Pseudomonas*, *Macrococcus*, *Brochothrix*, and Enterobacteriaceae, while *Leuconostoc*, *Latilactobacillus*, and *Duganella* were detected with less than 1% abundance (Table S3). Of note, *Janthinobacterium* spp. had low abundance in culturing but were the second most abundant genus in a floor trap sample incubated at 4 °C. This finding and the high frequency of uncultured *Janthinobacterium* isolates (Fig. 3) emphasize the necessity of using different culture conditions to recover this organism.

Strain-level analysis of dispersal within the facility and persistence over time

The species level composition of microbial communities on meat and in environmental samples (Figs. 2, 4, and 5) suggests that bacteria on meat originate from the facility. To provide further evidence for this hypothesis, and to document strain-level dispersal within the facility and persistence over time, we identified isolates at the strain level. First, core genome phylogenetic trees were generated of all species that were isolated from stored meat samples, i.e., *Carnobacterium*, *Rahnella*, and *Serratia* (Fig. 8 and Fig. S5). Pairwise SNP analysis was then used to identify closely related isolates at the strain level (Tables 2 and S5). The high relatedness of isolates from fresh and stored meats, 0–2 SNPs (Table 2), is expected as sampling likely isolated the same strain and thus validates the workflow for genome sequencing and SNP calling.

Figure 9 depicts the isolates from various sampling sites that differ in fewer than 10 SNPs on a schematic map of the processing facility. These isolates were considered

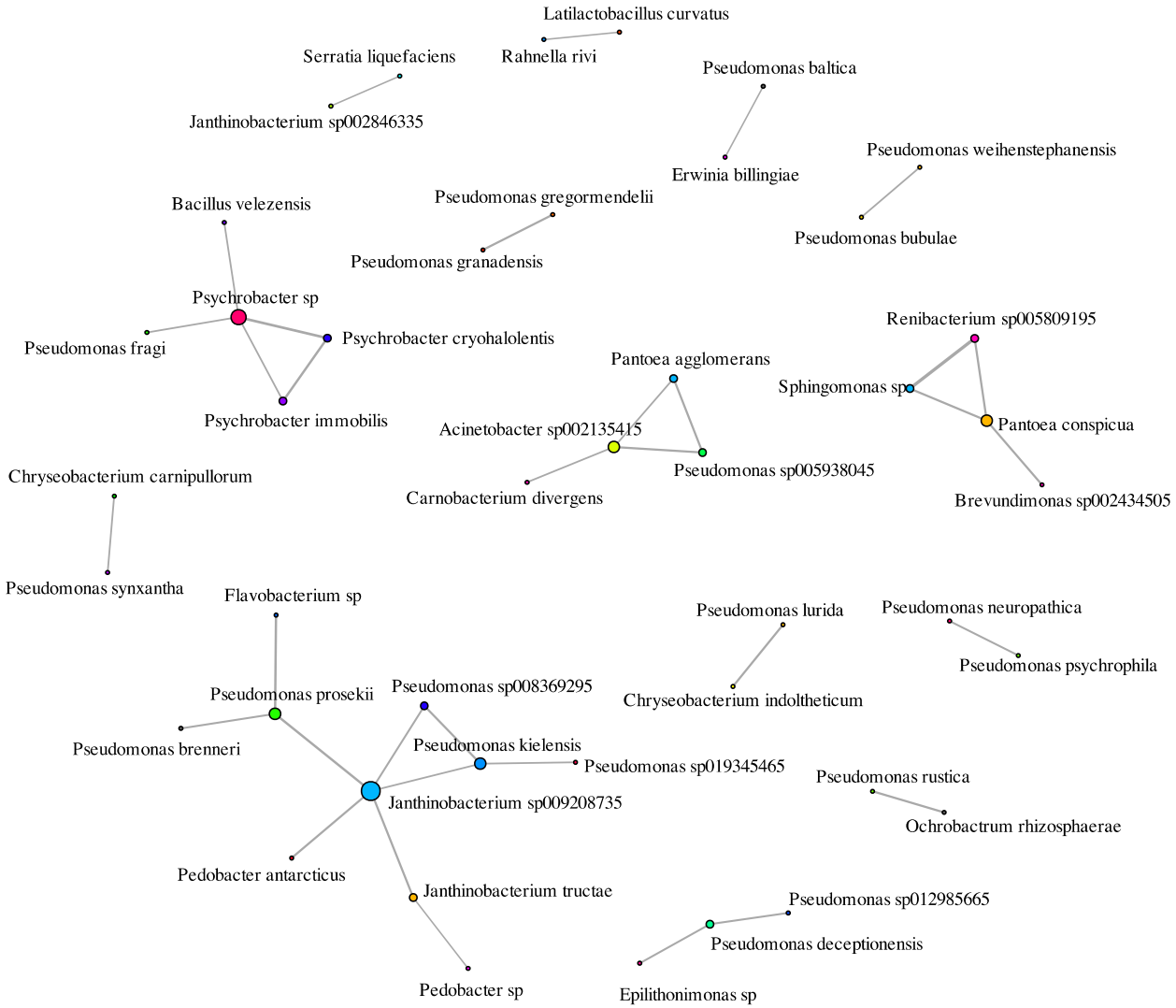

Fig. 6 Bacterial coexistence network based on the microbial communities across 66 surface samples and 4 meat samples, comprising 1281 isolates classified by genome sequencing. Bacterial species with one-time occurrence among all sampling surfaces were not included. Nodes are colored at species level. The network connections are determined using Spearman correlation test. Only correlations with a significance level of $p < 0.0001$ and a coefficient of > = 0.5 are included

to represent the same strain. Strains of all of species of interest were isolated at both sampling points (Table 2 and Table S5). Figure 9 thus indicates how spoilage-associated microbes dispersed across environmental surfaces and meat samples at a strain level. Notably, none of the strains was detected in the killing room, which was sampled only at one site. Isolates of *C. maltaromaticum* from fresh and stored meat samples were closely related to isolates from drain samples in the cooler room, a sanitized conveyor belt, the working table, or the vacuum packaging machine (Figs. 8 and 9).

Isolates of *Carnobacterium divergens* from the same meat sample pre- and post-storage were identical and matched other environmental isolates, which has persisted over 6 months regardless of sanitation measures (Fig. S5A and Table S5). Different strains of *C. divergens* dispersed across various environmental surfaces in the packaging area. For example, isolates from the conveyor belt (D-Trim 5 (T5)) differed by fewer than 4 SNPs from those on the equipment surface (ES3), quality control table, shrink tunnel, and working table (Fig. 9).

One drain isolate of *Rahnella rivi* collected post sanitation during the first-time sampling differed by 3 SNPs from isolates identified in the stored picnic sample from the second sampling. Meat isolate, *Rahnella inusitata* MC41 from the first sampling, differed by 3 or fewer

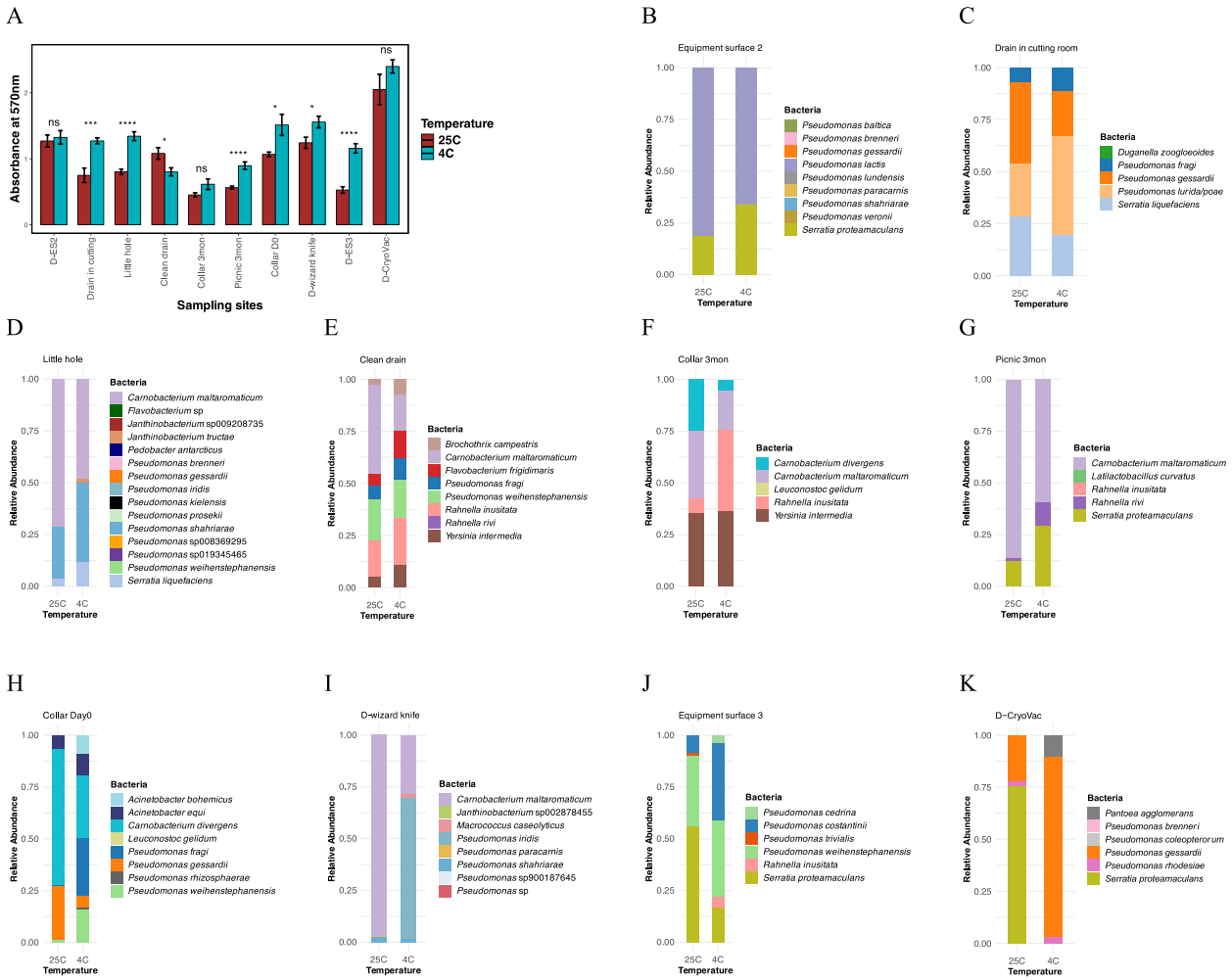

Fig. 7 Quantification of the biomass (**A**) and composition of the microbial community (**B**, **C**, **D**, **E**, **F**, **G**, **H**, **I**, **J**, **K**) of biofilms that were reconstituted with isolates from 10 sampling sites. Multispecies biofilms were grown at 4 °C and 25 °C in LBNS broth for 6 days before staining with crystal violet and accessing growth. Bacterial composition of biofilms from four non-food contact surfaces (**B** D-ES2, **C** drain in cutting room, **D** little hole (floor trap), **E** clean drain), three meat samples (**F** Collar 3mon, **G** Picnic 3mon, **H** Collar Day0), and three food-contact surfaces (**I** D-wizard knife, **J** D-ES3, **K** D-Cryovac) was evaluated. The experiment was repeated with three biological replicates, and mean value of cell counts was used to determine the relative abundance of each taxon. *T*-test was used to determine the biomass difference within each sampling site. Significance levels are indicated as follows: ns ($p > 0.05$), * ($p < 0.05$), *** ($p < 0.001$), and **** ($p < 0.0001$). Results of the sequence-based analysis of the same biofilm communities are shown in Table S4

SNPs from isolates collected from the conveyor belt and the break table in the second sampling. One isolate of *R. inusitata* from D-tray (TC1041) transmitted to other stored meat samples (< 2 SNPs).

Isolates of *Serratia proteamaculans*, differed by 2 SNPs, were found among meat isolates, non-food contact surfaces (NFCSs) such as quality control tables and drains, and food contact surfaces (FCSs) such as conveyor belts (D-CB#2) over a period of 6 months (Table S5). Two isolates that were collected from the same sampling site (D-ES3) over a period of 6 months differed by 2 SNPs. These isolates also differed by fewer than 5 SNPs from an environmental isolate from D-ES2 (NFCS of the Cryovac machine) and the Cryovac machine (D-Trim 5 (T5)). Taken together, meat isolates of *C. maltaromaticum* and *R. rivi* mainly originated from the drain area in cooler room, while meat isolates of *C. divergens* and *S. proteamaculans* dispersed and persisted both food contact and non-food contact surfaces in the packaging area.

Table 2. Pairwise single-nucleotide polymorphisms (SNPs) between genomes of isolates of *C. maltaromaticum* within the same phylogenetic cluster. Strain IDs are color coded vertically by isolates collected in the first sampling (light blue) and the second sampling (pink) or horizontally based on isolates from meat samples (purple), food contact surface (red), and non-food contact surface (sky blue). In each pairwise comparison, genome with a higher coverage was used as the reference

	SX455	MC12	L6	TC1285	TC1253	P4	P18	P15
SX455	-							
MC12	38	-						
L6	34	25	-					
TC1285	35	33	34	-				
TC1253	35	1	1	28	-			
P4	35	28	28	33	1	-		
P18	35	<1	<1	<1	1	<1	-	
P15	33	1	1	1	2	1	<1	-

	L3	P16	P1
L3	-		
P16	<1	-	
P1	<1	<1	-

	MC11	TC650	TC966
MC11	-		
TC650	10	-	
TC966	8	2	-

	TC922	TC807
TC922	-	
TC807	2	-

	TC1275	TC219
TC1275	-	
TC219	<1	-

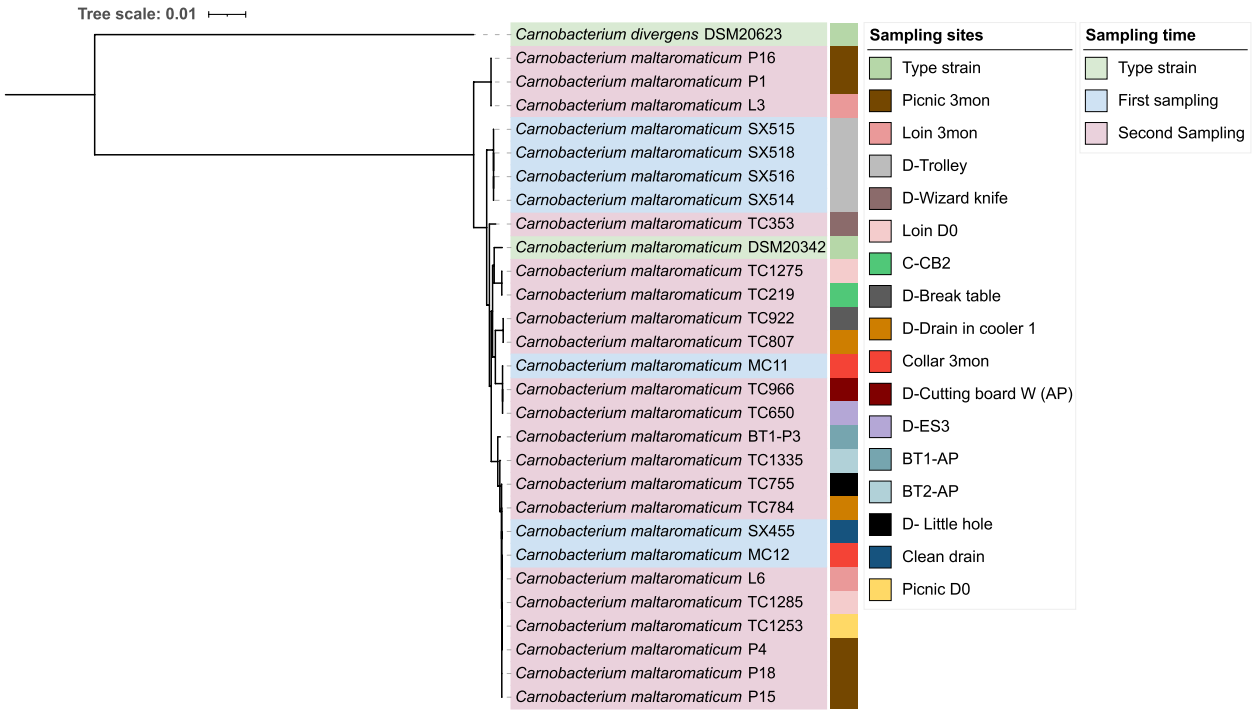

Fig. 8 Phylogenetic tree of strains of *C. maltaromaticum* based on core genome alignment, utilizing the GTR + I + G4 model with 1000 bootstrap replicates. The tree was rooted with the outgroup, *C. divergens* DSM20263. Strains are color coded based on sampling time or type strain (clades) and 16 sampling sites (color legend). The type strain *C. maltaromaticum* DSM 20342 was utilized for tree visualization

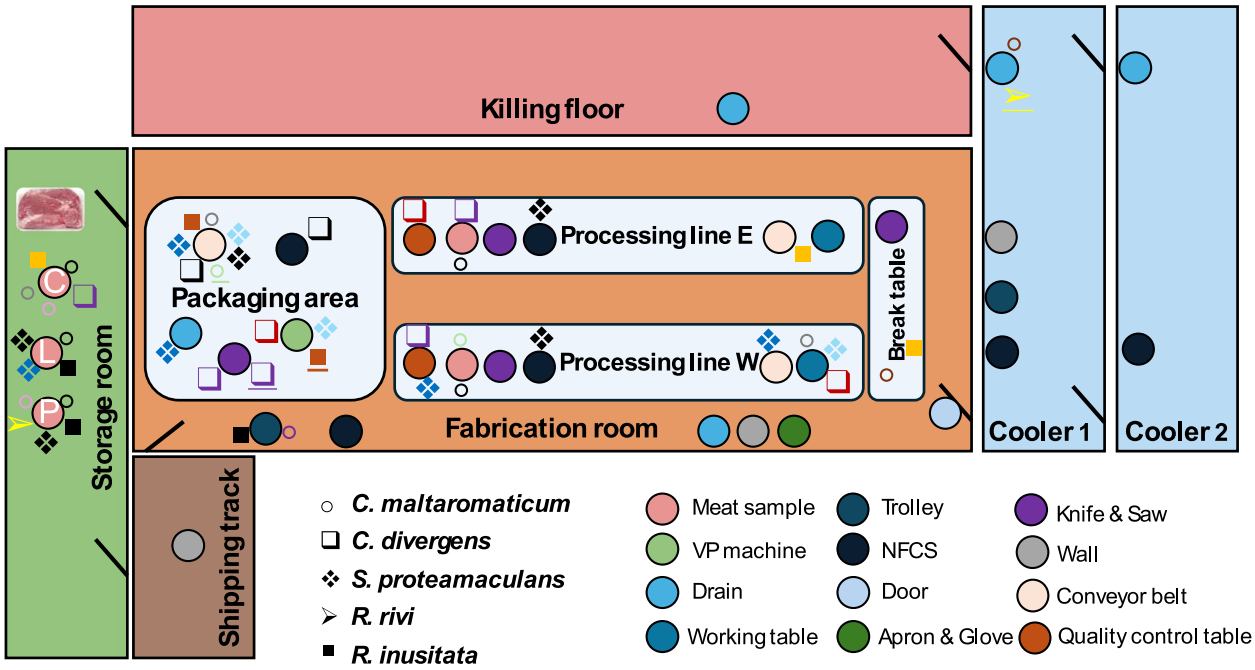

Fig. 9 Distribution of meat spoilage-associated isolates across various sampling sites from the meat processing facility. The symbols represent different bacterial species: *C. maltaromaticum* (○), *C. divergens* (❑), *S. proteamaculans* (❖), *R. rivi* (➢), and *R. inusitata* (■). The type of sampling site is color coded as in the figure. Underlined symbols denote isolates collected after cleaning and sanitation. Only isolates with fewer than 10 SNPs are shown. Isolates of the same strain dispersed across the facility are labeled with the same color symbols. FCS, food contact surfaces; *NFCS*, non-food contact surfaces. Processing line E operates muscle meat samples including leg, collar, and picnic, while processing line W is mainly for tenderloin and loin meat

Discussion

High-throughput culture-dependent and culture-independent analysis of microbiome dynamics in the meat processing facility

Sequence-based approaches are fast, affordable, and also accounted for microbes that occur in low abundance or are difficult to cultivate. However, 16S rRNA amplicon sequencing typically characterizes bacterial communities at the genus level and is subject to biases introduced by DNA extraction and PCR amplification [25]. In addition, DNA-based analyses do not differentiate between viable and dead cells [26, 27], which is particularly relevant for post-sanitation surfaces. Metagenomic sequencing is additionally constrained by the limitation of current reference databases and by contamination in low-biomass samples [28], although these constraints have been partially addressed by using appropriate sequencing depth, controls, and suitable protocols, e.g., by propidium monoazide treatment or by sequencing of RNA rather than DNA [8, 29, 30]. Culture-based methods used to identify bacteria in food processing facilities focused on foodborne pathogens and employed selective media to enumerate or isolate *L. monocytogenes*, *E. coli* O157:H7, and *Salmonella* [22, 31].

We employed a high-throughput culture-based approach in combination with sequencing of full-length 16S rRNA gene amplicons. Complementing this high-throughput culture-based approach with genome sequencing enabled us to characterize isolates at the strain level and thus to identify their persistence and dispersal in the facility. The culture-independent approach identified significantly more bacterial taxa, with the exception of *Janthinobacterium* and *Dellaglioa*; however, dominant taxa identified by sequencing were also detected by the culture-dependent methods. *Janthinobacterium* species was isolated from the drains of a food processing facility [32] and spoiled MAP-packaged broiler meat [33]. *Dellaglioa* species have been identified in various meat samples [34–37], but their role in spoilage is unclear. Knowledge on this organism is limited because culture media for cultivation of *Dellaglioa* spp. were published only in 2024 [38]. Conversely, 41 genera that were identified by culture represented fewer than 1% of the total sequencing reads. Therefore, obtaining cultured isolates is essential to expand the database of reference genomes and for subsequent physiological characterization as documented by high-throughput culture-based analyses of the gut microbiome [39, 40], plant roots [41], and marine samples [42]. Taken together, the

combination of both sequence-based and culture-based method is necessary to accurately represent the structure of the microbial communities in food processing facilities.

Microbial diversity in the meat processing facility

The meat processing facility harbored diverse microbial communities which include 74 bacterial taxa that were not previously cultured or characterized. A recent in-depth metagenomic analysis of meat processing plants revealed a comparable diversity of uncultured bacteria taxa [8], but without isolates, this diversity cannot be fully characterized. Isolates with high abundance and occurrence include representatives of genera that were frequently found within the meat processing environment such as *Pseudomonas*, *Acinetobacter*, *Psychrobacter*, and *Flavobacterium* which are also considered to spoil fresh meat [12]. Common representatives on vacuum-packaged meat, such as lactic acid bacteria (*Carnobacterium*, *Leuconostoc*, and *Latilactobacillus*), *Brochothrix*, and Enterobacteriaceae (*Serratia*, *Rahnella*, and *Hafnia*), were also found on environmental surfaces in the meat processing facility. Animal-associated microbes, such as *Clostridium*, *Clostridioides*, *Escherichia*, *Prevotella*, *Bacteroides*, and *Treponema* [43], were absent in both meat and environmental surface samples, supporting the prior conclusions that core microbiome across different food communities primarily originates from the processing facilities rather than the respective raw materials [12]. Remarkably, the composition of microbial communities in meat processing facilities partially overlaps with the composition of microbial communities in hospital environments [30], indicating that the observation of a core microbiome in food processing facilities [12] partially extends to other human-made environments that are sanitized regularly.

Meat spoilage-associated microbes are prevalent in the reconstituted biofilm communities

Reconstruction of model communities allows for a deeper understanding of microbial interactions in biofilm consortia [44, 45]. Biofilms provide an ecological niche for bacterial coexistence and cooperation and protect microbes against routine cleaning and sanitation, thus supporting persistence [10, 46]. Past studies have predominantly focused on biofilm formation in single and dual species, with only a few recent studies investigating bacterial interactions and composition in the reconstituted multispecies biofilms of environmental isolates, typically within an incubation temperature range of 7 to 15 °C [46–50]. We documented the ability of environmental isolates to form biofilm at refrigerated temperature (4 °C). The ability of forming biofilms at refrigerated temperature increases risks associated with psychrotrophic pathogens, such as *L. monocytogenes*. We also observed that one microbial community formed surface-attached biofilms at ambient temperature but floating pellicles at refrigeration temperature. Pellicle formation in *Acinetobacter baumannii* and *Pseudomonas aeruginosa* is associated with cyclic diguanylate (c-di-GMP) [51, 52], whose signal transduction is temperature dependent [53]. The switch of biofilm phenotypes also depends in interspecies communication [54]. Thus, the collection of isolates also allows further comprehensive research on microbial interactions and resistance to sanitation of biofilm-embedded microbes.

Strain-level characterization of dispersal within the facility and persistence over time

Studies on strain-level bacterial persistence in food processing facilities focused on pathogens [22, 55, 56], documenting strain-level persistence over a period of 17 years [18]. In investigations of foodborne outbreaks, a threshold of 21 SNPs is widely used for strain-level identification [16]. Most studies on persistence of *Listeria* in food processing facilities used the same SNP threshold [40–44]. However, *L. monocytogenes* evolved in a cold-smoked salmon processing facility with a mutation rate of only 0.35 SNPs per genome per year [18]. In addition to the environmental conditions including nutrient availability or environmental stress, the bacterial mutation rate depends on the bacterial species and the time of observation [57]. The SNP threshold for strain-level identification thus depends on the context [58, 59]. The cutoff of 21 SNPs is supported by tens of thousands of sequenced genomes in outbreak investigations [16], but such calibration data is unavailable for persisting spoilage microbes. In addition, bioinformatic workflows that were developed for Illumina-sequenced genomes do not perform well for SNP calling of genomes that were sequenced on the nanopore platform [58]. The bioinformatic tools for SNP calling of nanopore-sequenced genomes were developed very recently [58], and the present study is among the first to use these for identification of bacteria that are associated with food or food processing facilities [60]. We thus used a conservative SNP threshold of 10 SNPs, three times higher than the number of false positives of the SNP calling workflow, to achieve strain-level identification. The suitability of the bioinformatic tools used and the SNP threshold is supported by the high relatedness of isolates from the same batch of fresh and stored meats.

Meat processing facilities are exposed to a constant influx of bacteria from animals, water, air, and workers. Colonization by external microbes and persistence is determined by dispersal and selection, respectively [61]. Bacterial dispersal can be limited by control of incoming

bacteria from animals, air, water, and employees, while the persistence of bacteria is determined by nutrient availability, resistance to cleaning, and sanitation as well as biofilm formation [12]. Our study indicates that microbes dispersed spatially across surfaces and meat samples within the facility and persisted over 6 months. Our data together with literature data on persistence of *L. monocytogenes* indicates that microbial persistence in food processing facilities is the rule rather than an exception. The packaging area and floor drains in the cooler emerged as "hotspots" for bacterial persistence and subsequent transmission to meat samples. Common hypotheses to explain persistence includes biofilm formation, stress resistance, and inappropriate design of facilities and equipment [62]. Potential mechanisms of bacterial dispersal in food processing facilities include the product flow, turbulent flow of air, movement of workers, and cleaning and sanitation measures particularly high-pressure cleaning which creates aerosols [63] or dry ice blasting [64] which disperses surface-attached bacteria through sublimation of carbon dioxide. Our study provides the basis for future studies that elucidate the contribution of these mechanisms of bacterial dispersal in more detail.

In conclusion, despite the development and feasibility of culture-independent sequencing approaches in studying microbial ecology and diversity, Robert Koch's assertion that "a pure culture is the foundation of all research" remains relevant [65] when appropriately complemented with sequenced-based tools. The combination of high-throughput culture-dependent and culture-independent methods captured the diversity of microbes and demonstrated bacterial persistence in the processing facility. This finding provides evidence that food processing facilities are an establishment niche for spoilage bacteria. Prior studies document that pathogens including Shiga-toxin-producing *E. coli* and *L. monocytogenes* can also become established in food processing facilities [18, 56]. The prevalence of spoilage-associated isolates in synthetic biofilm communities suggests that biofilm formation contributes to persistence within the facility. These findings enhance our knowledge on source tracking of microbial food spoilage and promote the development of improved intervention strategies in food processing facilities and to extend the shelf life of meat and meat products.

Material and method

Sampling strategy

The sampling plan was conducted in a pork processing facility located in Alberta, Canada, producing packed fresh pork with a shelf life of 3 months for oversea shipment. Sampling activities were carried out in September 2022 and March 2023 (Fig. 1) in various rooms such as kill floor (15 °C), cooler (−3 to −1 °C), fabrication room (1 to 4 °C), storage room (1 °C), shipping truck (1 °C), and packaging area (1 °C). We considered the sampling time as experimental unit; thus, $n=2$, and the data on the composition of microbial communities in the processing facility provides qualitative, not quantitative results. To investigate as many different sites as possible at different conditions and how the microbial composition overlaps with meat productions, sampling was performed on both non-food contact surfaces (NFCS) and food contact surfaces (FCS) during operation hours, after cleaning and disinfection, and after production (AP). Environmental surface samples collected after sanitation are denoted with letter "C (clean)," environmental sampling sites collected during and after production are denoted with letter "D (dirty)," and samples collected after production are referred to as "AP." Meat samples were obtained directly from the production line and swabbed. Subsequently, meat samples were vacuum-packed and stored at 1 °C for a duration of 3 months, reflecting the anticipated shelf life, prior to sample collection. In total, 14 NFCS, 30 FCS, and 2 meat samples were collected during the first sampling, while 32 NFSC, 37 FCS, and 4 meat samples were collected during the second sampling. A standardized surface area of approximately 600 cm^2 was swabbed using pre-moistened Whirl–Pak® Speci-Sponge® Environmental Surface Sampling Bag (Sigma Aldrich, St. Louis, USA). All sponge samples were kept in a bag at 4 °C for further processing within 24 h.

Bacterial isolation and DNA extraction

To each sponge sample, 10 ml of 0.1% peptone water was added. The sponge sample was massaged from outside the bag for 2 min to homogenize [66]. The swab fluid was diluted and plated on plate count agar, all-purpose Tween agar, and VRBG agar to enumerate total aerobic bacteria, lactic acid bacteria, and coliforms, respectively. Plates were incubated at 25 °C for 72 h for cell counts determination and colony isolation. A total of 9 samples did not yield any culturable isolates (6 samples from first-time sampling and 3 samples from second-time sampling), and isolates are thus available for only 40 samples from the first-time sampling and 70 samples from second-time sampling.

To characterize the isolates, 2–5 representative colonies for each distinct colony morphology were streaked on corresponding plates. The number of colonies streaked was equal to or exceeded the square root of the total number of colonies on the plate. Repeated streak was performed until a uniform colony morphology was achieved. Isolates were subcultured into liquid medium to prepare for DNA extraction and frozen culture stocks

of 30% glycerol and stored at − 80 °C. Genomic DNA of each isolate was extracted using the Qiagen Blood & Tissue Kit (Qiagen, Hilden, Germany) following the manufacturer's protocol for gram-positive bacteria, which also recovers DNA from gram-negative bacteria. DNA concentration and purity were assessed using the NanoDrop spectrophotometer (Thermo Fisher Scientific). Clonal isolates within each sponge sample were determined by Random Amplified Polymorphic DNA PCR using Rep5 primer (GTG GTG GTG GTG GTG). PCR was performed with genomic DNA as the template in a reaction volume of 25 µl containing 1-µl genomic DNA, 12.5-µl DreamTaq Master Mix, 1-µl 50-mM MgCl2, and 1-µl 100 nmol Rep5 primer. Thermocycler conditions were set to the following: 1 min of incubation at 96 °C; 3 cycles of 3 min at 96 °C, 5 min at 35 °C, and 5 min at 75 °C; and 32 cycles of 1 min at 96 °C, 2 min at 55 °C, 3 min at 75 °C, and 2 min at 75 °C. RAPD PCR products were separated on 1% agarose gel (60 V, 2.5 h) and were visualized by UV transillumination after staining with SYBR Safe.

To capture the microbial community in each sponge sample by 16S rRNA gene sequencing, 1 ml of sponge swab fluid was used to extract the community DNA using the DNeasy Blood & Tissue kit, following the manufacturer's instructions for extracting DNA from gram-positive bacteria. Three negative extraction controls without any bacterial pellets were also included. The quality and quantity of the extracted DNA were determined using a NanoDrop spectrophotometer. In total, 42 out of 46 sponge samples collected in September 2022 and 66 out of 70 sponge samples collected in March 2023 met the input DNA quality requirements for nanopore 16S gene sequencing. The PCR amplification (according to 16S Barcoding Kit 1–24 (SQK-16S024) protocol) did not yield amplicons of 16S rRNA genes for those eight low-biomass samples; thus, these samples were not included in the sequencing approach.

Genome sequencing

To achieve the species identification, isolates from the first sampling were identified based on the 16S rRNA gene by Sanger sequencing. The 16S rRNA gene region was amplified using primers 27F (5′-AGA GTT TGA TCM TGG CTC AG-3′) and 1492R (5′- GGY TAC CTT GTT ACG ACT T-3′) with the following thermocycler condition: initial denaturation at 95 °C for 5 min, followed by 30 cycles of denaturation at 95 °C for 30 s, annealing at 60 °C for 10 s, and elongation at 72 °C for 90 s, with a final extension step at 72 °C for 10 min. PCR products underwent gel electrophoresis (1.5%) for quality control and were subsequently purified using the Qiagen QIAquick PCR Purification Kit (Qiagen, Hilden, Germany) before Sanger sequencing. Forward and reverse nucleotide sequences were manually inspected and corrected using SnapGene Viewer, followed by alignment using EMBOSS prior to blasting against the NCBI database and RDP classifier training set no. 19 to achieve species-level taxonomic assignment [67].

For isolates obtained in the second sampling, the protocol for sequence-based identification was modified owing to advances in the Oxford Nanopore Whole Genome sequencing platform. DNA concentration was reassessed using the dsDNA broad-range assay kits for the Qubit 4 Fluorometer (Thermo Fisher Scientific, Schwerte, Germany). The protocol started with 450-ng input DNA per isolate. DNA library was prepared following the protocol of Native Barcoding Kit 96 V14 (SQK-NBD114.96) and loaded onto R10.4.1 MinION flow cell. Raw data were basecalled by Guppy baseballer, and genome was assembled by following the nextflow epi2me/wf-bacterial-genome workflow. The genome coverage ranges from 5 to 70, with a mean coverage of 18 among 1052 sequenced genomes. Taxonomy classification was determined by Genome Taxonomy Database Toolkit (GTDB-Tk v2.4.0) based on Genome Taxonomy Database [68].

Additionally, microbial composition and diversity of each meat and environmental sample were analyzed by nanopore full-length 16S rRNA gene sequencing. DNA libraries were prepared using the 16S Barcoding Kit 1–24 (SQK-16S024) protocol and sequenced on R 9.4.1 Flongle flow cells. Raw data were basecalled by Guppy basecaller, with the use of model "dna_r9.4.1_450bps_hac." Subsequently, epi2me-labs/wf-16Ss workflow was used to blast against "ncbi_16s_18s" database, and only read length between 1200 and 1800 bp were kept for taxonomy classification.

Biofilm formation

Ten sites which include *Carnobacterium* and *Serratia* species were chosen to reconstitute multiple-species biofilms and assess their microbial community composition and biofilm formation. Frozen (− 80 °C) stock cultures of bacterial isolates were streaked onto Luria–Bertani agar plates and incubated in a 25 °C incubator for 48 h, followed by subculture in Luria–Bertani without NaCl (LBNS) broth at 25 °C for an additional 48 h without agitation. A preliminary assessment was conducted to optimize biofilm formation over 2, 4, and 6 days, with the most robust biofilm formation observed after 6 days of incubation. To simulate the meat processing environment, multispecies biofilms were cultivated on food-grade stainless steel coupons (grade 304, No. 4 finish, 12-mm diameter; Stanfos, Edmonton, AB, Canada) at both 4 and 25°, following the established protocol [7]. Briefly, overnight cultures of each isolate were standardized to ensure equal bacterial populations. One milliliter

each standardized overnight culture was then combined together and mixed by vortexing to create an overnight culture cocktail. This cocktail was then diluted 100-fold in 2 ml of LBNS suspension. Stainless steel (SS) coupons were placed into the bottom of a 24-well flat-bottom cell culture plate (Corning, Glendale, Arizona), and the 2-ml diluted bacterial suspension was transferred into each well. The plate was incubated at 4 °C and 25 °C for 6 days. After 6 days of incubation, biofilms grown on SS coupons were harvested and used for cell counts determination and biomass quantification. Cell counts were determined after gently washing of the coupons to remove loosely attached planktonic cells. Biofilm-embedded cells were detached by vortexing with glass beads at maximum speed for 1 min. One milliliter of detached-biofilm suspension was used for differential cell counts of each isolate based on their bacterial morphology on LB agar, APT agar, and *Yersinia* selective agar, and the other aliquot (1 ml) was used for DNA extraction and nanopore 16S full-length sequencing, as described above. Biofilm biomass was quantified with crystal violet staining by following the established protocol [7] and measured as absorbance at 570 nm using plate reader (Varioskan Flash, Thermo Fisher Scientific). Three independent experiments with technical duplicates were conducted ($n=3$) for microbial composition determination and biofilm biomass quantification.

Phylogenetic and single-nucleotide polymorphism (SNP) analysis

Phylogenetic analysis was conducted on all isolates of species that were isolated from meat after 3 months of refrigerated storage, including *C. maltaromaticum*, *C. divergens*, *R. rivi*, *R. inusitata*, and *S. proteamaculans*. Sequencing libraries with the Nanopore Native Barcoding Kit V14 on the Nanopore MinION R10.4.1 flow cell aimed to achieve a 100-fold to 200-fold higher coverage. Raw data in pod5 format were subset to extract information on read ID and channel using the Pod5 package v0.3.10 (available at https://github.com/nanoporetech/pod5-file-format). Subsequently, data were basecalled by Dorado basecaller (available at https://github.com/nanoporetech/dorado) with the basecalling model of dna_r10.4.1_e8.2_400bps_sup@v4.3.0 and demultiplexed by Dorado demux to achieve per barcoded groups. The barcoded sample was basecalled using Dorado duplex. Basecalled reads were filtered by Chopper (NanoPack) [69] to retain those with a quality score of at least 20 and a read length of at least 500 bp. Porechop_ABI v0.5.0 [70] was employed to trim adapter sequences and enhance quality. Read quality was assessed after filtering and adapter trimming using the FastQC program (available at https://www.bioinformatics.babraham.ac.uk/projects/fastqc/). Post-QC reads were de novo assembled using Flye v2.9.3 [71] with 0.03 read error rate and polished with Medaka v1.11.3 (available at https://github.com/nanoporetech/medaka). Prokka v1.14.5 [72] was used for genome annotation, and core genome was aligned by Roary [73], with the minimum percentage identity for Blastp set at 90%. The aligned sequences were further filtered through TrimAL v1.2 [74]. A maximum likelihood (ML) phylogenetic tree was constructed based on the core gene alignment using RAxML-NG v1.12.1 [75]. ModelTest-NG v0.1.7 [76] was employed to predict the best nucleotide substitution model and bootstrap replicate values. The resulting phylogenetic tree was visualized using iTOL [77] and refined by Inkscape. The accession numbers of all genomes used for the phylogenetic analysis are provided in Table S6.

FastANI (v1.34) was used for whole-genome pairwise alignment [78], and only isolates with over 99.90% ANI value were taken for SNP analysis [79]. Firstly, post-QC reads underwent mapping against assembled reference genome with Minimap2 via the epi2me-labs /wf-alignment workflow. Subsequently, SNPs were called using variant caller Clair3 v1.0.7 [80] with a recently described workflow [60]. The pairwise SNP matrix table was generated using genomes with a higher coverage as the reference. Additional parameters were configured to tailor the SNP calling process: All contigs were considered in the analysis. Phasing by WhatsHap was omitted during full alignment calling. Haploid mode was enabled, wherein only the presence of 1/1 was regarded as indicative of a variant. Lastly, only candidates passing SNP minimum allele frequency (AF) threshold were considered, while indel candidates were ignored. Output results were visualized on Integrative Genomic Viewer (IGV 2.17.2) and manually checked to eliminate false-positive variants. The following criteria were used to eliminate false-positive variants: (i) indels were eliminated, (ii) the quality score was lower than 2, and (iii) the variant distance bias was at least 0.00001 [81].

Statistical analysis

Data visualization and statistical analysis were performed in R environment (v4.3.1). Bacterial diversity was assessed using permutational multivariate analysis of variance (PERMANOVA, 999 permutations, adonis2 function, *vegan* package, R v4.3.0) based on the Bray–Curtis dissimilarity of bacterial communities with an error probability of 5% ($p \leq 0.05$) to determine whether sampling areas from different type of surfaces, location, sanitation activity, and zones harbored different communities of microbes. The data were visualized by principal coordinate analysis (PCoA). Pairwise comparisons between groups were tested by the "pairwise.adonis" function

(*pairwiseAdonis* package (v0.4.1)) [82] with Bonferroni adjustment [83] for multiple comparisons. A total of 795,396 reads were generated for samples collected in second sampling with an average of 12,051 sequencing reads per sample. Prior to Spearman's rank correlation analysis, samples with fewer than 1000 reads were excluded from further analysis. This cutoff was determined based on a preliminary rarefaction curve analysis using *vegan* package (v2.6.6) [84]. Spearman's rank correlation was performed to infer the co-occurrence of bacterial isolates with the use of *psych* package (v 2.4.3) [85]. The correlation with p-value less than 0.01 and absolute value coefficient > 0.5 was considered as significant. The microbial network analysis was then created and visualized using *igraph* package (v2.0.3) [86]. T-test was used to determine the significant difference in biomass of each sampling site between growth condition at 25 °C and 4 °C.

Abbreviations

SS	Stainless steel
AP	After production
NFCS	Non-food contact surface
FCS	Food contact surface
PCA	Plate count agar
APT	All-purpose Tween
VRBG	Violet red bile glucose
LBNS	Luria–Bertani without NaCl
GTDB	Genome Taxonomy Database
SNP	Single-nucleotide polymorphism
ANOVA	Analysis of variance
PCoA	Principal coordinates analysis
PCR	Polymerase chain reaction
PERMANOVA	Permutational multivariate analysis of variance

Supplementary Information

The online version contains supplementary material available at https://doi.org/10.1186/s40168-024-02026-1.

Additional file 1. Figure S1. Heatmap of bacterial isolates collected from meat samples, environmental surface samples during the first time sampling, September 2022. Figure S2. Relative abundance of uncultured genera that were only detected by 16S sequencing, among samples collected in the first sampling, September 2022. Figure S3. Principal coordinate analysis, using Bray–Curtis distance with 605 isolates classified at species level for 40 sampling sites, collected at the first sampling time, September 2022. Figure S4. Bacterial coexistence network based on the microbial communities characterized by 16S rRNA gene sequencing. Figure S5. Phylogenetic tree of strains of C. divergens (A), Rahnella (B) and S. proteamaculans (C) isolated from a meat processing facility.

Additional file 2. Table S1. List of sites that were sampled in September 2022 (provided as excel file). Table S2. List of sites that were sampled in March 2023 (provided as excel file). Table S3. Permutational multivariate analysis of variance on Bray–Curtis distance matrix of samples in March 2023 by both culture-dependent and culture-independent approaches. Table S4. Bacterial relative abundance in biofilm samples determined by 16S rRNA sequencing. Only taxa with a relative abundance of 1% r more are presented (provided as excel file). Table S5. Pairwise single nucleotide polymorphisms (SNPs) matrix for isolates of *C. divergens*, *R. rivi*, *R. inusitata* and *S. proteamaculans*. Only isolates with more than 99% ANI value were included for SNP variant analysis (provided as excel file). Table S6. Strains used for phylogenetic analyses and multi-species biofilm reconstitution in this study. The table also includes NCBI Accession Numbers for genomes that were sequenced with high coverage and used in the phylogenetic analyses and SNP calling (provided as excel file).

Acknowledgements
The authors would like to express their gratitude to the management and staff in the pork processing facility of Sunterra Meats of Trochu, Alberta, that participated in the study. We are also thankful to Dr. Dirk Thiele of Ensolucion, Austin, TX, USA, for his assistance with the on-site sampling.

Authors' contributions
SZX: Methodology, Formal analysis, Investigation, Data Curation, Writing - Original Draft, Writing - Review & Editing, Visualization. VDP: Methodology, Writing - Review & Editing. XQY: Conceptualization, Writing - Review & Editing, Supervision, Funding acquisition. MGG: Conceptualization, Methodology, Data Curation, Writing - Original Draft, Writing - Review & Editing, Visualization, Supervision, Project administration, Funding acquisition.

Funding
Zhaohui Shaelyn Xu acknowledges Mitacs Accelerate and Sunterra Meats for funding. The project (PI's Gänzle and Yang) is funded by RDAR (2023F239R) with support from Sunterra Meats and En Solución. Michael Gänzle acknowledges support from the Canada Research Chairs Program.

Data availability
Sequence data for bacterial genomes, 16S rRNA gene sequences obtained from community DNA of samples from the meat processing facility, and 16S rRNA gene sequences obtained from re-constituted biofilm communities are available from NCBI. The raw reads in FASTQ format from Nanopore 16S sequencing of the 113 community DNA samples and 20 synthetic biofilm samples, as well as the genome FASTA files from the whole genome sequencing of 82 isolates, are available under NCBI BioProject ID PRJNA1138274. The bacterial genomes of BioSample accession numbers range from SAMN42689982 to SAMN42690063. The BioSample accession numbers for the raw reads FASTQ files of community samples range from SAMN42780823 to SAMN42780935, and those for synthetic biofilm samples range from SAMN42783738 to SAMN42783757. The link to the sequence archives is (release date Oct 30, 2024 or acceptance of the manuscript): https://dataview.ncbi.nlm.nih.gov/object/PRJNA1138274?reviewer=3ifhf8n9r952os6cutloqub0uu.

Declarations

Ethics approval and consent to participate
Not applicable.

Consent for publication
Not applicable.

Competing interests
The authors declare no competing interests.

Received: 17 July 2024 Accepted: 30 December 2024
Published online: 27 January 2025

References

1. Klaura J, Breeman G, Scherer L. Animal lives embodied in food loss and waste. Sustain Prod Consum. 2023;43:308–18.
2. Yang X, Narvaez-Bravo C, Zhang P. Driving forces shaping the microbial ecology in meat packing plants. Front Microbiol. 2023;14:1333696.
3. Yang X, McMullen LM. Factors affecting microbial spoilage. In: Dikeman M, editor. Encyclopedia of Meat Sciences, 3rd Ed. Cambridge: Academic Press; 2023. p. 219–28.
4. Gill CO. Sources of microbial contamination at slaughtering plants. Improv Saf Fresh Meat. 2005;:231–43.

5. Snyder AB, Martin N, Wiedmann M. Microbial food spoilage: impact, causative agents and control strategies. Nat Rev Microbiol. 2024;2024:1–15.
6. Fagerlund A, Langsrud S, Møretrø T. Microbial diversity and ecology of biofilms in food industry environments associated with *Listeria monocytogenes* persistence. Curr Opin Food Sci. 2021;37:171–8.
7. Xu ZS, Yang X, Gänzle MG. Resistance of biofilm-and pellicle-embedded strains of *Escherichia coli* encoding the transmissible locus of stress tolerance (tLST) to oxidative sanitation chemicals. Int J Food Microbiol. 2021;359: 109425.
8. Barcenilla C, Cobo-Díaz JF, Puente A, Valentino V, De Filippis F, Ercolini D, et al. In-depth characterization of food and environmental microbiomes across different meat processing plants. Microbiome. 2024;12:199.
9. Flemming H-C, Wingender J, Szewzyk U, Steinberg P, Rice SA, Kjelleberg S. Biofilms: an emergent form of bacterial life. Nat Rev Microbiol. 2016;14:563–75.
10. Alvarez-Ordóñez A, Coughlan LM, Briandet R, Cotter PD. Biofilms in food processing environments: challenges and opportunities. Annu Rev Food Sci Technol. 2019;10:173–95.
11. Jespersen L, Huffman R. Building food safety into the company culture: a look at Maple Leaf Foods. Perspect Public Health. 2014;134:200–5.
12. Xu ZS, Ju T, Yang X, Gänzle M. A meta-analysis of bacterial communities in food processing facilities: driving forces for assembly of core and accessory microbiomes across different food commodities. Microorganisms. 2023;11: 1575.
13. Casaburi A, Nasi A, Ferrocino I, Di Monaco R, Mauriello G, Villani F, et al. Spoilage-related activity of *Carnobacterium maltaromaticum* strains in air-stored and vacuum-packed meat. Appl Environ Microbiol. 2011;77:7382–93.
14. Podlesny D, Arze C, Dörner E, Verma S, Dutta S, Walter J, et al. Metagenomic strain detection with SameStr: identification of a persisting core gut microbiota transferable by fecal transplantation. Microbiome. 2022;10:53.
15. Van Rossum T, Ferretti P, Maistrenko OM, Bork P. Diversity within species: interpreting strains in microbiomes. Nat Rev Microbiol. 2020;18:491–506.
16. Pightling AW, Pettengill JB, Luo Y, Baugher JD, Rand H, Strain E. Interpreting whole-genome sequence analyses of foodborne bacteria for regulatory applications and outbreak investigations. Front Microbiol. 2018;9:1482.
17. Holt RD. Bringing the Hutchinsonian niche into the 21st century: ecological and evolutionary perspectives. Proc Natl Acad Sci. 2009;106(Supplement 2):19659–65.
18. Harrand AS, Jagadeesan B, Baert L, Wiedmann M, Orsi RH, Dudley EG. Evolution of *Listeria monocytogenes* in a food processing plant involves limited single-nucleotide substitutions but considerable diversification by gain and loss of prophages. Appl Environ Microbiol. 2020;86:e02493–519.
19. Alvarez-Molina A, Cobo-Díaz JF, López M, Prieto M, de Toro M, Alvarez-Ordóñez A. Unraveling the emergence and population diversity of *Listeria monocytogenes* in a newly built meat facility through whole genome sequencing. Int J Food Microbiol. 2021;340:109043.
20. Daeschel D, Pettengill JB, Wang Y, Chen Y, Allard M, Snyder AB. Genomic analysis of *Listeria monocytogenes* from US food processing environments reveals a high prevalence of QAC efflux genes but limited evidence of their contribution to environmental persistence. BMC Genomics. 2022;23:488.
21. Tassinari E, Duffy G, Bawn M, Burgess CM, McCabe EM, Lawlor PG, et al. Microevolution of antimicrobial resistance and biofilm formation of *Salmonella* Typhimurium during persistence on pig farms. Sci Rep. 2019;9:1–12.
22. Arthur TM, Bono JL, Kalchayanand N. Characterization of *Escherichia coli* O157: H7 strains from contaminated raw beef trim during " high event periods ." Appl Environ Microbiol. 2014;80:506–14.
23. Zwirzitz B, Wetzels SU, Dixon ED, Fleischmann S, Selberherr E, Thalguter S, et al. Co-occurrence of Listeria spp. and spoilage associated microbiota during meat processing due to cross-contamination events. Front Microbiol. 2021;12:632935.
24. FDA. Control of Listeria monocytogenes in ready-to-eat foods: guidance for industry. 2017. p. 1–79. https://www.fda.gov/regulatory-information/search-fda-guidance-documents/draft-guidance-industry-control-listeria-monocytogenes-ready-eat-foods. Accessed 16 May 2024.
25. Laursen MF, Dalgaard MD, Bahl MI. Genomic GC-content affects the accuracy of 16S rRNA gene sequencing bsed microbial profiling due to PCR bias. Front Microbiol. 2017;8: 287367.
26. Wuyts S, Van Beeck W, Oerlemans EFM, Wittouck S, Claes IJJ, De Boeck I, et al. Carrot juice fermentations as man-made microbial ecosystems dominated by lactic acid bacteria. Appl Environ Microbiol. 2018;84:e00134-e218.
27. Ruan H, Wu Y, Zhang N, Tao Y, Wang K, Yan B, et al. *Serratia marcescens* causes the brown discoloration of frozen steamed stuffed buns during resteaming. J Agric Food Chem. 2024;72:4991–5002.
28. Kennedy KM, de Goffau MC, Perez-Muñoz ME, Arrieta MC, Bäckhed F, Bork P, et al. Questioning the fetal microbiome illustrates pitfalls of low-biomass microbial studies. Nature. 2023;613:639–49.
29. Wang Y, Thompson KN, Yan Y, Short MI, Zhang Y, Franzosa EA, et al. RNA-based amplicon sequencing is ineffective in measuring metabolic activity in environmental microbial communities. Microbiome. 2023;11:1–15.
30. Shen J, McFarland AG, Blaustein RA, Rose LJ, Perry-Dow KA, Moghadam AA, et al. An improved workflow for accurate and robust healthcare environmental surveillance using metagenomics. Microbiome. 2022;10:1–18.
31. Ferreira V, Barbosa J, Stasiewicz M, Vongkamjan K, Switt AM, Hogg T, et al. Diverse geno- and phenotypes of persistent *Listeria monocytogenes* isolates from fermented meat sausage production facilities in Portugal. Appl Environ Microbiol. 2011;77:2701–15.
32. Fox EM, Solomon K, Moore JE, Wall PG, Fanning S. Phylogenetic profiles of in-house microflora in drains at a food production facility: comparison and biocontrol implications of *Listeria*-positive and -negative bacterial populations. Appl Environ Microbiol. 2014;80:3369–74.
33. Lauritsen CV, Kjeldgaard J, Ingmer H, Bisgaard M, Christensen H. Microbiota encompassing putative spoilage bacteria in retail packaged broiler meat and commercial broiler abattoir. Int J Food Microbiol. 2019;300:14–21.
34. Cauchie E, Delhalle L, Taminiau B, Tahiri A, Korsak N, Burteau S, et al. Assessment of spoilage bacterial communities in food wrap and modified atmospheres-packed minced pork meat samples by 16S rDNA metagenetic analysis. Front Microbiol. 2020;10: 483567.
35. Hultman J, Johansson P, Björkroth J, Drake HL. Longitudinal metatranscriptomic analysis of a meat spoilage microbiome detects abundant continued fermentation and environmental stress responses during shelf life and beyond. Appl Environ Microbiol. 2020;86:e01575–620.
36. Jääskeläinen E, Hultman J, Parshintsev J, Riekkola ML, Björkroth J. Development of spoilage bacterial community and volatile compounds in chilled beef under vacuum or high oxygen atmospheres. Int J Food Microbiol. 2016;223:25–32.
37. Pothakos V, Snauwaert C, De Vos P, Huys G, Devlieghere F. Psychrotrophic members of *Leuconostoc gasicomitatum*, *Leuconostoc gelidum* and *Lactococcus piscium* dominate at the end of shelf-life in packaged and chilled-stored food products in Belgium. Food Microbiol. 2014;39:61–7.
38. Werum V, Ehrmann M. Dellaglioa spp. an underestimated genus isolated from high-oxygen modified-atmosphere packaged meat. Food Microbiol. 2024;117: 104398.
39. Forster SC, Kumar N, Anonye BO, Almeida A, Viciani E, Stares MD, et al. A human gut bacterial genome and culture collection for improved metagenomic analyses. Nat Biotechnol. 2019;37:186–92.
40. Zou Y, Xue W, Luo G, Deng Z, Qin P, Guo R, et al. 1,520 reference genomes from cultivated human gut bacteria enable functional microbiome analyses. Nat Biotechnol. 2019;37:179–85.
41. Zhang J, Liu YX, Guo X, Qin Y, Garrido-Oter R, Schulze-Lefert P, et al. High-throughput cultivation and identification of bacteria from the plant root microbiota. Nat Protoc. 2021;16:988–1012.
42. Joint I, Mühling M, Querellou J. Culturing marine bacteria - an essential prerequisite for biodiscovery: minireview. Microb Biotechnol. 2010;3:564–75.
43. Quan J, Wu Z, Ye Y, Peng L, Wu J, Ruan D, et al. Metagenomic characterization of intestinal regions in pigs with contrasting feed efficiency. Front Microbiol. 2020;11: 32.
44. O'Toole GA. We have a community problem. J Bacteriol. 2024;206:e00073-e00124.
45. Shayanthan A, Ordoñez PAC, Oresnik IJ. The role of synthetic microbial communities (SynCom) in sustainable agriculture. Front Agron. 2022;4: 896307.
46. Sadiq FA, De Reu K, Steenackers H, Van de Walle A, Burmølle M, Heyndrickx M. Dynamic social interactions and keystone species shape the diversity and stability of mixed-species biofilms – an example from dairy isolates. ISME Commun. 2023;3:118.

47. Fagerlund A, Møretrø T, Heir E, Briandet R, Langsruda S. Cleaning and disinfection of biofilms composed of *Listeria monocytogenes* and background microbiota from meat processing surfaces. Appl Environ Microbiol. 2017;83:e01046–117.
48. Rolon ML, Voloshchuk O, Bartlett KV, LaBorde LF, Kovac J. Multi-species biofilms of environmental microbiota isolated from fruit packing facilities promoted tolerance of *Listeria monocytogenes* to benzalkonium chloride. Biofilm. 2024;7: 100177.
49. Wang R, Guragain M, Chitlapilly Dass S, Palanisamy V, Bosilevac JM. Impact of intense sanitization on environmental biofilm communities and the survival of *Salmonella enterica* at a beef processing plant. Front Microbiol. 2024;15: 1338600.
50. Langsrud S, Moen B, Møretrø T, Løype M, Heir E. Microbial dynamics in mixed culture biofilms of bacteria surviving sanitation of conveyor belts in salmon-processing plants. J Appl Microbiol. 2016;120:366–78.
51. Ahmad I, Nygren E, Khalid F, Myint SL, Uhlin BE. A cyclic-di-GMP signalling network regulates biofilm formation and surface associated motility of *Acinetobacter baumannii* 17978. Sci Rep. 2020;10:1–11.
52. Li Z, Chen JH, Hao Y, Nair SK. Structures of the PelD cyclic diguanylate effector involved in pellicle formation in *Pseudomonas aeruginosa* PAO1. J Biol Chem. 2012;287:30191–204.
53. Almblad H, Randall TE, Liu F, Leblanc K, Groves RA, Kittichotirat W, et al. Bacterial cyclic diguanylate signaling networks sense temperature. Nat Commun. 2021;12:1986.
54. Xu ZS, Zhu T, Wang Z, Yang X, Gänzle MG. Socializing at the air-liquid interface: a functional genomic analysis on biofilm-related genes during pellicle formation by *Escherichia coli* and its interaction with *Aeromonas australiensis*. Appl Environ Microbiol. 2023;89:e00456–523.
55. Estrada EM, Harris LJ. Phenotypic characteristics that may contribute to persistence of *Salmonella* strains in the pistachio supply shain. J Food Prot. 2024;87: 100268.
56. Yang X, He A, Badoni M, Tran F, Wang H. Mapping sources of contamination of *Escherichia coli* on beef in the fabrication facility of a commercial beef packing plant. Food Control. 2017;75:153–9.
57. Kuo CH, Ochman H. Inferring clocks when lacking rocks: the variable rates of molecular evolution in bacteria. Biol Direct. 2009;4: 35.
58. Pham VD, Simpson DJ, Gänzle MG. Strain-level identification of bacteria persisting in food and in food processing facilities: when do two isolates represent the same strain and which tools identify a strain? Curr Opin Food Sci. 2025;61: 101245.
59. Wang Y, Pettengill JB, Pightling A, Timme R, Allard M, Strain E, et al. Genetic diversity of *Salmonella* and *Listeria* isolates from food facilities. J Food Prot. 2018;81:2082–9.
60. Pham VD, Xu SZ, Simpson DJ, Zhang J, Gänzle MG. Does strain-level persistence of lactobacilli in long term back-slopped sourdoughs inform on domestication of food-fermenting lactic acid bacteria? Appl Environ Microbiol. 2024;:e01892–24.
61. Vellend M. Conceptual synthesis in community ecology. Q Rev Biol. 2010;85:183–206.
62. Ferreira V, Wiedmann M, Teixeira P, Stasiewicz MJ. *Listeria monocytogenes* persistence in food-associated environments: epidemiology, strain characteristics, and implications for public health. J Food Prot. 2014;77:150–70.
63. Saini JK, Marsden JL, Fung DYC, Crozier-Dodson BA. Evaluation of potential for translocation of *Listeria monocytogenes* from floor drains to food contact surfaces in the surrounding environment using *Listeria innocua* as a surrogate. Adv Microbiol. 2012;2:565–70.
64. Witte AK, Bobal M, David R, Blättler B, Schoder D, Rossmanith P. Investigation of the potential of dry ice blasting for cleaning and disinfection in the food production environment. LWT. 2017;75:735–41.
65. Brock TD. Robert Koch: A Life in Medicine and Bacteriology. Am Soc Microbiol. 1999;64:475–6.
66. Yang X, Wang H, Hrycauk S, Klassen MD. Effects of peroxyacetic acid spray and storage temperature on the microbiota and sensory properties of vacuum-packed subprimal cuts of meat. Appl Environ Microbiol. 2021;87:e03143–220.
67. Wang Q, Cole JR. Updated RDP taxonomy and RDP Classifier for more accurate taxonomic classification. Microbiol Resour Announc. 2024;13:e01063–123.
68. Chaumeil PA, Mussig AJ, Hugenholtz P, Parks DH. GTDB-Tk v2: memory friendly classification with the genome taxonomy database. Bioinformatics. 2022;38:5315–6.
69. De Coster W, Rademakers R. NanoPack2: population-scale evaluation of long-read sequencing data. Bioinformatics. 2023;39: btad311.
70. Bonenfant Q, Noe L, Touzet H. Porechop_ABI: discovering unknown adapters in Oxford Nanopore Technology sequencing reads for downstream trimming. Bioinforma Adv. 2023;3:vbac085.
71. Kolmogorov M, Yuan J, Lin Y, Pevzner PA. Assembly of long, error-prone reads using repeat graphs. Nat Biotechnol. 2019;37:540–6.
72. Seemann T. Prokka: rapid prokaryotic genome annotation. Bioinformatics. 2014;30:2068–9.
73. Page AJ, Cummins CA, Hunt M, Wong VK, Reuter S, Holden MTG, et al. Roary: rapid large-scale prokaryote pan genome analysis. Bioinformatics. 2015;31:3691–3.
74. Capella-Gutiérrez S, Silla-Martínez JM, Gabaldón T. TrimAl: a tool for automated alignment trimming in large-scale phylogenetic analyses. Bioinformatics. 2009;25:1972–3.
75. Kozlov AM, Darriba D, Flouri T, Morel B, Stamatakis A. RAxML-NG: a fast, scalable and user-friendly tool for maximum likelihood phylogenetic inference. Bioinformatics. 2019;35:4453–5.
76. Darriba D, Posada D, Kozlov AM, Stamatakis A, Morel B, Flouri T. ModelTest-NG: a new and scalable tool for the selection of DNA and protein evolutionary models. Mol Biol Evol. 2020;37:291–4.
77. Letunic I, Bork P. Interactive Tree Of Life (iTOL) v5: an online tool for phylogenetic tree display and annotation. Nucleic Acids Res. 2021;49:W293–6.
78. Jain C, Rodriguez-R LM, Phillippy AM, Konstantinidis KT, Aluru S. High throughput ANI analysis of 90K prokaryotic genomes reveals clear species boundaries. Nat Commun. 2018;9:5114.
79. Rodriguez-R LM, Conrad RE, Viver T, Feistel DJ, Lindner BG, Venter SN, et al. An ANI gap within bacterial species that advances the definitionsdefinitionsof intra-species units. MBio. 2024;15: e02696.
80. Zheng Z, Li S, Su J, Leung AWS, Lam TW, Luo R. Symphonizing pileup and full-alignment for deep learning-based long-read variant calling. Nat Comput Sci. 2022;2:797–803.
81. Hall MB, Rabodoarivelo MS, Koch A, Dippenaar A, George S, Grobbelaar M, et al. Evaluation of nanopore sequencing for *Mycobacterium tuberculosis* drug susceptibility testing and outbreak investigation: a genomic analysis. The Lancet Microbe. 2023;4:e84-92.
82. Martinez Arbizu P. pairwiseAdonis: pairwise multilevel comparison using adonis. 2020. https://github.com/pmartinezarbizu/pairwiseAdonis.
83. Armstrong RA. When to use the Bonferroni correction. Ophthalmic Physiol Opt. 2014;34:502–8.
84. Oksanen J, Simpson GL, Blanchet FG, Kindt R, Legendre P, Minchin PR, et al. Community ecology package [R package vegan version 2.6–8]. CRAN Contrib Packag. 2024. https://doi.org/10.32614/CRAN.PACKAGE.VEGAN.
85. Revelle W. Procedures for psychological, psychometric, and personality research [R package psych version 2.4.6.26]. CRAN Contrib Packag. 2024. https://doi.org/10.32614/CRAN.PACKAGE.PSYCH.
86. Csárdi G, Nepusz T, Traag V, Horvát S, Zanini F, Noom D, et al. Network analysis and visualization [R package igraph version 2.1.2]. CRAN Contrib Packag. 2024. https://doi.org/10.32614/CRAN.PACKAGE.IGRAPH.

Publisher's Note